Asian Journal of Chemistry; Vol. 33, No. 1 (2021), 83-88

ASIAN JOURNAL OF CHEMISTRY

https://doi.org/10.14233/ajchem.2021.22922

Spectroscopic, Electronic and Optical Properties of 4-Nitroimidazole using DFT Calculations

S. JEYAVIJAYAN[1,*] and PALANI MURUGAN[2]

[1]Department of Physics, Kalasalingam Academy of Research and Education, Anand Nagar, Krishnankoil-626126, India
[2]Department of Physics, Dr. B.R. Ambedkar Institute of Technology, Port Blair-744103, India

*Corresponding author: E-mail: sjeyavijayan@gmail.com

Received: 4 August 2020; *Accepted*: 22 September 2020; *Published online*: 10 December 2020; AJC-20181

Theoretical and experimental vibrational spectra of 4-nitroimidazole were studied by FTIR, FT-Raman spectroscopic techniques and density functional theory (DFT) method. The contributions of the different modes to each wavenumber were confirmed using total energy distribution (TED). The optimized parameters and thermodynamic properties of 4-nitroimidazole have been computed. The charge transfer interactions of the molecule were explained from the small value of HOMO-LUMO energy gap. The NBO analysis, Mulliken's plot and MEP studies of the molecule have also been reported.

Keywords: 4-Nitroimidazole, Total energy distribution, DFT calculations, FT-Raman.

INTRODUCTION

Nitroimidazoles are key molecules with extensive range of activity and therapeutic potential. A plethora of nitroimidazole based drugs are available for the treatment of bacterial and protozoal borne infections [1]. They belong to a group of nitroheterocyclic compounds that have broad spectrum activity against a series of organisms such as mycobacteria, anaerobic Gram-positive and Gram-negative bacteria and some of them have already been used in clinics or under clinical trials for the treatment of infectious diseases [2]. Further, imidazole derivatives acted as energetic materials for civil and military applications when they have more than two nitro groups [3], specifically 4-nitroimidazole. Due to its significant features in recent times, numerous experimental and theoretical studies have been made on the vibrational spectra of imidazole derivatives [4-6]. The vibrational spectra reveal the exact biological process and the complex process, which takes place in the imidazole derivatives. Further, among DFT calculations, Becke's three parameter hybrids functional combined with the Lee-Yang-Parr correlation functional (B3LYP) is the best in expecting outcomes for molecular geometry and vibrational wavenumbers even for larger molecular structures indicating conformity of higher level between the experimental and the calculated results [7]. In the DFT methodology, numerous exchange and correlation functionals are normally used. In the present investigation, complete B3LYP comparative report on the vibrational spectra of 4-nitroimidazole was performed to derive information about its electronic effects and intramolecular charge transfer.

EXPERIMENTAL

The FTIR was studied at room temperature in the region 4000-400 cm^{-1} using Perkin Elmer FTIR spectrometer equipped with an MCT detector, a KBr beam splitter and globar source. The FT-Raman spectrum of molecule was recorded on a Bruker/RFS-100/S model interferometer using accessories of FT-Raman (FRA-106) in the Stokes region 4000-50 cm^{-1} (for excitation 1064 nm line Nd:YAG laser source at 150 mW power). The accuracy of the wavenumbers was maintained within ± 4 cm^{-1}.

The quantum chemical density functional calculations converged for the minimum energy optimized geometry. The 2009 Window version of the GAUSSIAN suite program [8] using Becke-3-Lee-Yang-Parr (B3LYP) functionals [9,10] supplemented with the standard B3LYP/6-311++G(d,p) basis set is used to calculate quantum chemical density functional. Scaled quantum mechanical (SQM) method [11] ensures the better agreement between computational and the experimental data. The molecular geometrical parameters, frequencies and

This is an open access journal, and articles are distributed under the terms of the Attribution 4.0 International (CC BY 4.0) License. This license lets others distribute, remix, tweak, and build upon your work, even commercially, as long as they credit the author for the original creation. You must give appropriate credit, provide a link to the license, and indicate if changes were made.

electronic parameters are computed and the performance of the computational method for B3LYP is carried out based on SQM approach. The MOLVIB Program (Version V7.0-G77) by Sundius [12] has been used in the calculation of the total energy distribution (TED).

RESULTS AND DISCUSSION

Molecular geometry: The optimized molecular structure of 4-nitroimidazole belongs to C_s point group symmetry is shown in Fig. 1. The geometrical parameters calculated by B3LYP/6-311++ G(d,p) method along with the experimental X-ray diffraction data are shown in Table-1 and they are the sources for comp-uting other parameters [13]. As seen from the observation, the computed geometries from B3LYP method are consistent with the experimental values for 4-nitroimidazole. In the B3LYP/6-311++(d,p) calculation, the influence of conjugation between the nitro group and the imidazole ring system can be under-stood by the increase in bond length of C1-N9 (1.4236 by B3LYP and 1.420 Å by experimental). Due to the bond lengths C1–C2, C2-N7, C3-N7, C3-N4 and C1-N4 at the C-H substitution place, the ring looks to be imbalanced, which are calculated values as 1.3773, 1.3627, 1.3232, 1.3555 and 1.3738 Å, respectively (1.361, 1.349, 1.318, 1.348 and 1.363 Å by experimental). These bond lengths are smaller than the C1-N9 bond in the molecule. In the DFT calculations, the bond angles of C2-C1-N4, C1-C2-N7, N4-C3-N7 and C1-N4-C3 are computed as 106.70°, 109.23°, 112.03° and 106.07°, respectively, (Experimental values: 112.1°, 104.4°, 112.0° and 103.4°). This irregularity of the angles explains the significance of the repulsion between nitro group, C-H and the imidazole ring system. The minimum energy found by the DFT-B3LYP optimi-zation with the 6-311++G(d,p) basis sets for 4-nitroimidazole is -430.84393467 Hartrees. The thermodymanic parameters of 4-nitroimidazole are listed in Table-2. Higher the value of dipole moment stronger will be the intermolecular interaction. In this study, the calculated total energy and dipole moment of 4-nitroimidazole were found to be 50.015 kcal mol^{-1} and 3.7985 Debye, respectively. The insignificant zero point vibrational energy is obtained (46.215 kcal mol^{-1}) for 4-nitroimidazole. These parameters can be used to estimate directions of chemical reactions and also to compute other thermodynamic energies from the thermodynamic relative functions.

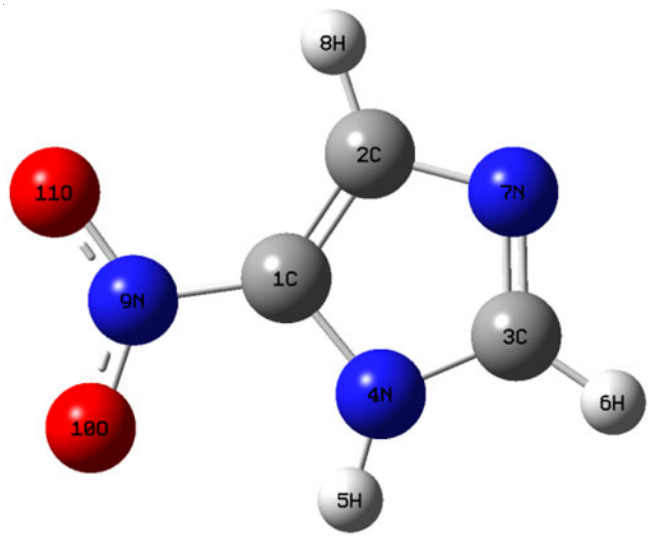

Fig. 1. Molecular structure of 4-nitroimidazole

TABLE-1
OPTIMIZED GEOMETRICAL PARAMETERS OF 4-NITROIMIDAZOLE OBTAINED BY DFT-B3LYP METHOD

Bond length (Å)	B3LYP/ 6-311++ G(d,p)	Expt. [17]	Bond angle (°)	B3LYP/ 6-311++ G(d,p)	Expt. [17]
C1-C2	1.3773	1.361	C2-C1-N4	106.70	112.1
C1-N4	1.3738	1.363	C2-C1-N9	132.30	126.9
C1-N9	1.4236	1.420	N4-C1-N9	121.01	120.8
C2-N7	1.3627	1.349	C1-C2-N7	109.23	104.4
C2-H8	1.0777	0.91	C1-C2-H8	127.80	130.0
C3-N4	1.3555	1.318	N7-C2-H8	122.97	118.0
C3-H6	1.0792	1.00	N4-C3-H6	122.51	125.0
C3-N7	1.3232	1.348	N4-C3-N7	112.03	112.0
N4-H5	1.0106	0.82	H6-C3-N7	125.47	129.0
N9-O10	1.2347	1.229	C1-N4-C3	106.07	103.4
N9-O11	1.2249	1.227	C1-N4-H5	124.56	132.0
			C3-N4-H5	129.37	120.0
			C2-N7-C3	105.97	108.0
			C1-N9-O10	116.74	118.5
			C1-N9-O11	117.77	118.4
			O10-N9-O11	125.49	123.0

TABLE-2
THEORETICALLY COMPUTED THERMODYNAMIC PARAMETERS OF 4-NITROIMIDAZOLE

Parameters	Method/Basis set B3LYP/6-311++G(d,p)
Optimized global minimum energy (Hartrees)	-430.84393467
Total energy (thermal), E_{total} (kcal mol^{-1})	50.015
Heat capacity, C_v (cal mol^{-1} k^{-1})	21.718
Entropy, S (cal mol^{-1} k^{-1})	
Total	79.150
Translational	40.083
Rotational	27.665
Vibrational	11.402
Vibrational energy, E_{vib} (kcal mol^{-1})	48.237
Zero point vibrational energy, (kcal mol^{-1})	46.215
Rotational constants (GHz)	
A	5.51086
B	1.70574
C	1.30257
Dipole moment (Debye)	3.7985

Vibrational assignments: 4-Nitroimidazole molecule possesses 11 atoms thus there are 27 normal modes of vibrations which are active in both Raman scattering and infrared absorption. The observed and calculated FTIR and FT-Raman spectra of 4-nitroimidazole are shown in Figs. 2 and 3, respectively and Table-3 reflects the normal mode descriptions (characterized by TED) for NIM along with the calculated IR and Raman intensities. Discrepancies occur between the observed and calculated vibrational wavenumbers because calculations are done on free molecule but experiments carried out with solid. Therefore, the calculated wavenumbers were scaled by using the scaling factor of 0.9613 for B3LYP method [14]. The scaled frequencies are listed in Table-3.

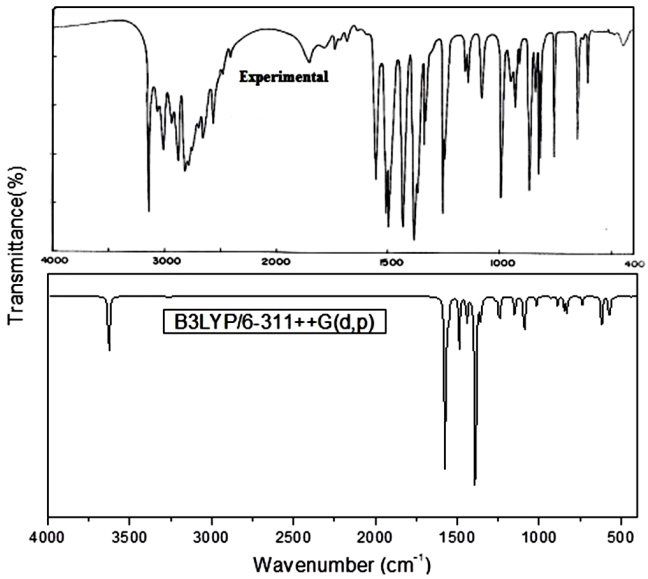

Fig. 2. Observed and calculated FTIR spectra of 4-nitroimidazole

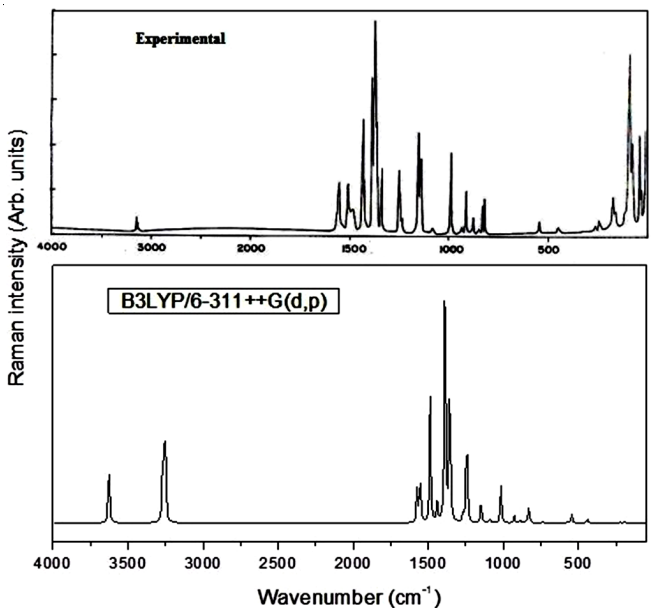

Fig. 3. Observed and calculated FT-Raman spectra of 4-nitroimidazole

N-H vibrations: The N-H stretching vibrations for heterocyclic compounds occur in the region 3500-3000 cm^{-1} [15], absorption in this region depends upon the degree of hydrogen bonding and physical state of the sample. Hence, in the present investigation, the N-H stretching vibrations have been found at 3452 cm^{-1} in IR as strong band for the title compound. The in-plane and out-of-plane bending vibrations of N-H group are also supported by the literature [16].

C-H vibrations: In 4-nitroimidazole, the scaled B3LYP/6-311++G(d,p) computed wavenumbers at 3141, 3126 cm^{-1} represents C-H stretching mode of vibrations (96% TED), since the characteristic region for the ready identification of C-H in hetero aromatic structure found in the region 3100-3000 cm^{-1} [17]. Similarly, the experimental values of both IR and Raman bands have been identified at 3135, 3138, 3122 cm^{-1}. The C-H in-plane and out-of-plane bending modes in 4-nitroimidazole are also found to be consistent with the calculated wave numbers as presented in Table-3.

C-N vibrations: There may be overlapping of many bands due to which the identification of C-N vibrations becomes complicated and hence the C-N stretching absorption is assigned in the region 1382-1266 cm^{-1} for aromatic compounds [18]. In 4-nitroimidazole, the band observed at 1372, 1332, 1190, 1102 and 1375, 1302 cm^{-1} in FTIR and Raman spectra, respectively, are assigned to C-N stretching vibration and the corresponding force constant contribute 72% to the TED. In this study, the bands observed at 598 cm^{-1} in IR spectrum is assigned to C-N in-plane bending vibration of 4-nitroimidazole. Due to the resonance of C-N bond with the ring, increases the force constants and slight shift in wavenumber. The out-of-plane C-N bending vibration has also been assigned and is listed in Table-3.

NO_2 vibrations: Each NO_2 group has six fundamentals associated to it namely, $NO_{2sym\ str.}$; $NO_{2asym\ str.}$; NO_{2sciss}; NO_{2rock}; NO_{2wag} and NO_{2twist} mode. Of these, the bands corresponding to scissoring, rocking, wagging and twisting vibrations of NO_2 groups found well within the characteristic region [19] and are summarized in Table-3. The NO_2 asymmetric stretching vibrations are normally observed in the region 1510-1485 cm^{-1}. In this work, the IR and Raman spectra of 4-nitroimidazole are detected at 1508 and 1510 cm^{-1}, respectively. The symmetric stretch usually appear between 1370 and 1320 cm^{-1} while in the experimental spectra for 4-nitroimidazole, NO_2 symmetric stretching is identified at 1420 and 1425 cm^{-1}.

HOMO-LUMO and Mulliken's population analysis: The HOMO and LUMO represent the ability to donate and accept an electron, respectively which decides the chemical stability of the molecule [20]. The 3D plots of the HOMO and LUMO computed at the B3LYP/6-311G++(d,p) level for NIM (in gas phase) are illustrated in Fig. 4. The energy gap between the HOMO and LUMO for 4-nitroimidazole were found to be 4.738 eV, which elucidates the charge transfer interactions occur in the molecule. In the HOMO-LUMO transition, an electron density transfer from nitro group to imidazole ring implies the charge redistribution and it influences vibrational spectra [21]. Hence, the atomic charges of 4-nitroimidazole were calculated by Mulliken population analysis with B3LYP method and corresponding plots of Mulliken's plot are shown in Fig. 5. From the result, it is clear that the substitution of NO_2 group in the aromatic imidazole ring leads to a redistribution of electron density. The carbon atom C1 bonded with the nitro group have the more negative charge (2.847) compare to other ring carbon atoms.

NBO analysis: The NBO investigation explains the conjugative interaction in molecular systems. Interactions between both filled and virtual orbital spaces improve the analysis of intra and inter molecular interactions [22]. The second-order Fock matrix was carried out to evaluate donor (i) and acceptor (j) interaction. A filled bonding or lone pair orbital can act as a donor. An empty or filled bonding, antibonding or lone pair orbital can act as an acceptor. These interactions can strengthen and weaken the bonds. For each donor (i) and acceptor (j), the stabilization energy (E_2) associates with the delocalization $i \rightarrow j$ is estimated as:

TABLE-3
OBSERVED FTIR, FT RAMAN AND CALCULATED (UNSCALED AND SCALED) FREQUENCIES (cm^{-1}), IR INTENSITY (Km mol^{-1}), RAMAN ACTIVITY ($Å^4$ amu^{-1}), REDUCED MASSES (amu) AND FORCE CONSTANT (m dyne $Å^{-1}$) AND PROBABLE ASSIGNMENTS (CHARACTERIZED BY TED) of 4-NITROIMIDAZOLE USING B3LYP METHOD

S. No.	Observed wavenumber (cm^{-1})		Calculated wavenumber (cm^{-1}) B3LYP/6-311++G(d,p)						Assignment (TED %)
	FTIR	FT-Raman	Unscaled	Scaled	Reduced mass	Force constant	IR intensity	Raman activity	
1	3452(s)	–	3627	3487	1.08	8.39	118.83	64.01	νNH (98)
2	3135(ms)	3138(w)	3267	3141	1.10	6.92	2.89	69.83	νCH (96)
3	3122(ms)	–	3252	3126	1.10	6.84	1.56	94.50	νCH (96)
4	1508(vs)	1510(ms)	1574	1513	11.35	16.58	268.15	18.64	NO_2ass (85)
5	1490(s)	1494(ms)	1555	1495	4.27	6.09	50.71	30.05	ν CC (72)
6	1420(s)	1425(s)	1487	1429	4.46	5.81	68.05	58.43	NO_2ss (74)
7	1372(s)	1375(ms)	1442	1386	3.46	4.24	42.87	11.49	ν CN (72)
8	1332(ms)	–	1388	1334	9.85	11.19	402.33	161.59	ν CN (72)
9	–	1302(ms)	1356	1304	5.73	6.22	42.29	82.98	ν CN (72)
10	1215(ms)	–	1268	1219	1.69	1.60	7.08	5.47	βNH (70)
11	1190(ms)	–	1243	1195	3.51	3.20	54.79	57.43	νCN (72)
12	1102(s)	–	1149	1105	1.68	1.31	37.25	11.94	νCN (72)
13	1050(vs)	1052(s)	1091	1049	1.50	1.06	77.58	2.22	βCH (76)
14	975(ms)	976(ms)	1017	978	4.76	2.90	15.65	17.74	βCH (77)
15	890(s)	888(w)	929	893	6.13	3.12	2.71	3.29	ωCH (65)
16	858(ms)	856(ms)	887	853	1.40	0.65	12.48	1.15	ωCH (63)
17	815(s)	–	846	813	1.43	0.60	18.80	0.90	ωNlH (62)
18	796(s)	–	829	797	12.29	4.99	27.67	7.59	NO_2sci (69)
19	702(s)	705(ms)	737	708	8.78	2.81	13.89	0.45	Rasymd (67)
20	–	652(ms)	675	649	2.04	0.55	0.00	0.31	Rsymd (65)
21	598(ms)	–	619	595	1.84	0.42	64.55	0.04	βBCN (61)
22	–	550(w)	571	549	2.77	0.53	48.70	0.38	τRsymd (58)
23	522(ms)	–	545	524	7.98	1.40	2.91	3.75	TRasymd (60)
24	422(w)	425(vw)	443	426	10.11	1.17	0.88	2.14	NO_2rock (63)
25	–	218(ms)	222	213	6.76	0.20	8.18	0.23	NO_2wag (62)
26	–	184(s)	191	184	7.66	0.16	3.59	0.68	ωCN (57)
27	–	102(ms)	104	100	7.31	0.05	3.04	0.02	τNO_2 (56)

ν-stretching; ss–symmetric stretching; β-bending; ω-out-of-plane bending; R-ring; symd-symmetric deformation; asymd-antisymmetric deformation; τ-torsion; s-strong; vs-very strong; ms-medium strong; w-weak; vw-very weak.

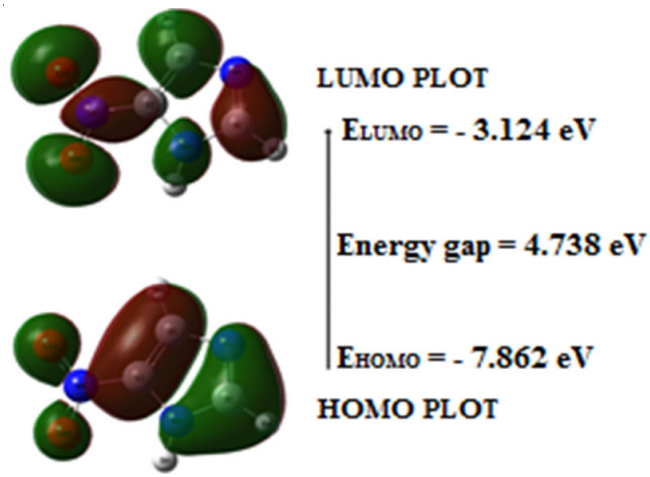

Fig. 4. HOMO-LUMO plot of 4-nitroimidazole

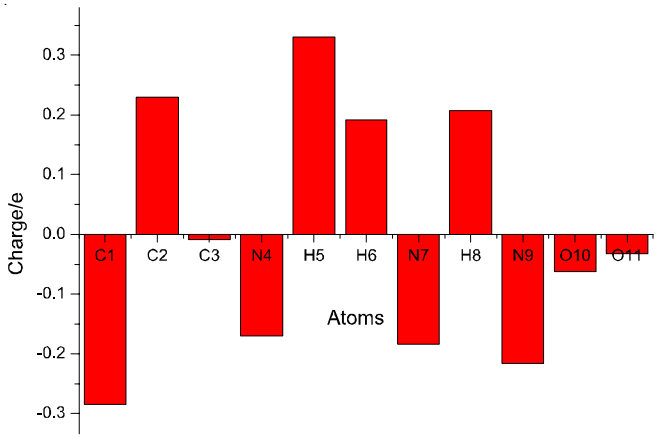

Fig. 5. Mulliken's plot of 4-nitroimidazole

$$E_2 = \Delta E_{ij} = q_i \frac{F(i,j)^2}{\varepsilon_i - \varepsilon_j}$$

where q_i is the donor orbital occupancy, ε_i and ε_j are diagonal elements and F(i,j) is the off diagonal NBO Fock matrix element. Larger the stabilization energy (E_2) value, the more intensive is the interaction between electron donors and acceptors *i.e.* the more donation tendency from electron donors to electron acceptor and greater the extent of conjugation of the whole system. In this study, the NBO analysis of 4-nitroimidazole has been performed at the DFT/B3LYP/6-311G++

(d,p) method in order to elucidate charge transfers or conjugative interaction, the intra molecular rehybridization and delocalization of electron density within the molecule. The second order perturbation theory analyses of Fock matrix in the NBO basis of 4-nitroimidazole are presented in Table-4. The n-π conjugation between the oxygen, nitrogen lone pair electrons and imidazole ring system is strong in the ground state. The orbital interaction in lone pair of nitrogen and oxygen atoms $\nu_2(N_7) \rightarrow \pi^*(C_3–N_4)$, $\nu_1(N_9) \rightarrow \sigma^*(O_{10}–O_{11})$ and $\nu_2(O_{10}) \rightarrow \sigma^*(C_1–N_9)$ results stabilization energies of 69.90, 472.23 and 7.60 kJ mol^{-1}, respectively. These interactions show n-σ, n-π conjugation between oxygen, nitrogen atoms and the imidazole ring. The interesting interactions in 4-nitroimidazole molecule is $\pi^*(C_3–N_4) \rightarrow \pi^*(C_1–C_2)$ which result the enormous stabilization energy of 9.97 kJ mol^{-1}. This highest interaction around the ring can induce the large bioactivity in the molecule. Hence, 4-nitroimidazole structure is stabilized by these orbital interactions.

Molecular electrostatic potential (MEP): In the present study, MEP analysis used to predict the electrophilic and nucleophilic attack [23] for 4-nitroimidazole by B3LYP/6-311++G(d,p) method and the pictorial representation is given in Fig. 6. In the MEP diagram, the potential energy increases from red < orange < yellow < green < blue. Other than the nitro functional group, the rest of the molecule contains the positive potential. Negative electrostatic potential (ESP) spread over the nitro functional group and is replicated as a yellowish blob. In MEP map, the negative potential sites are on oxygen atoms (red) of nitro group and the positive potential sites are around the hydrogen atoms of the molecule (blue). Furthermore, in 4-nitroimidazole, two concepts have been identified based on attraction and repulsion. The H atoms indicate the

TABLE-4
SECOND-ORDER PERTURBATION THEORY ANALYSIS OF FOCK MATRIX IN NBO BASIS FOR 4-NITROIMIDAZOLE

Donor (i)	ED (i) (e)	Acceptor (j)	ED (j) (e)	[a]E(2) (kJ mol^{-1})	[b]E(j)–E(i) (a.u.)	[c]F (i,j) (a.u.)
$\sigma(C_1–C_2)$	0.99279	$\sigma^*(N_4–H_5)$	0.00755	1.66	1.16	0.055
$\pi(C_1–C_2)$	0.88941	$\pi^*(C_3–N_4)$	0.30719	5.90	0.21	0.050
		$\sigma^*(O_{10}–O_{11})$	0.45998	1.15	0.03	0.010
$\sigma(C_2–N_7)$	0.98795	$\sigma^*(C_1–N_9)$	0.05465	3.15	0.99	0.072
$\sigma(C_3–N_4)$	0.99417	$\sigma^*(C_1–N_9)$	0.05465	2.26	1.08	0.064
$\pi(C_3–N_4)$	0.95744	$\pi^*(C_1–C_2)$	0.16817	7.94	0.36	0.072
$\nu_2(N_7)$	0.61777	$\pi^*(C_1–C_2)$	0.16817	23.01	0.18	0.091
		$\pi^*(C_3–N_4)$	0.30719	69.90	0.11	0.113
$\nu_1(N_9)$	0.58914	$\pi^*(C_1–C_2)$	0.16817	8.26	0.32	0.074
		$\sigma^*(O_{10}–O_{11})$	0.45998	472.23	0.07	0.238
$\nu_2(O_{10})$	0.94626	$\sigma^*(C_1–N_9)$	0.05465	7.60	0.56	0.082
		$\sigma^*(N_9–O_{11})$	0.02602	9.58	0.78	0.110
$\nu_2(O_{11})$	0.94364	$\sigma^*(C_1–N_9)$	0.05465	7.56	0.55	0.081
		$\sigma^*(N_9–O_{10})$	0.02740	9.74	0.77	0.111
$\pi^*(C_3–N_4)$	0.30719	$\pi^*(C_1–C_2)$	0.16817	9.97	0.07	0.049

[a]E(2) means energy of hyperconjugative interactions; [b]Energy difference between donor and acceptor i and j NBO orbitals; [c]F(i,j) is the Fock matrix element between i and j NBO orbitals.

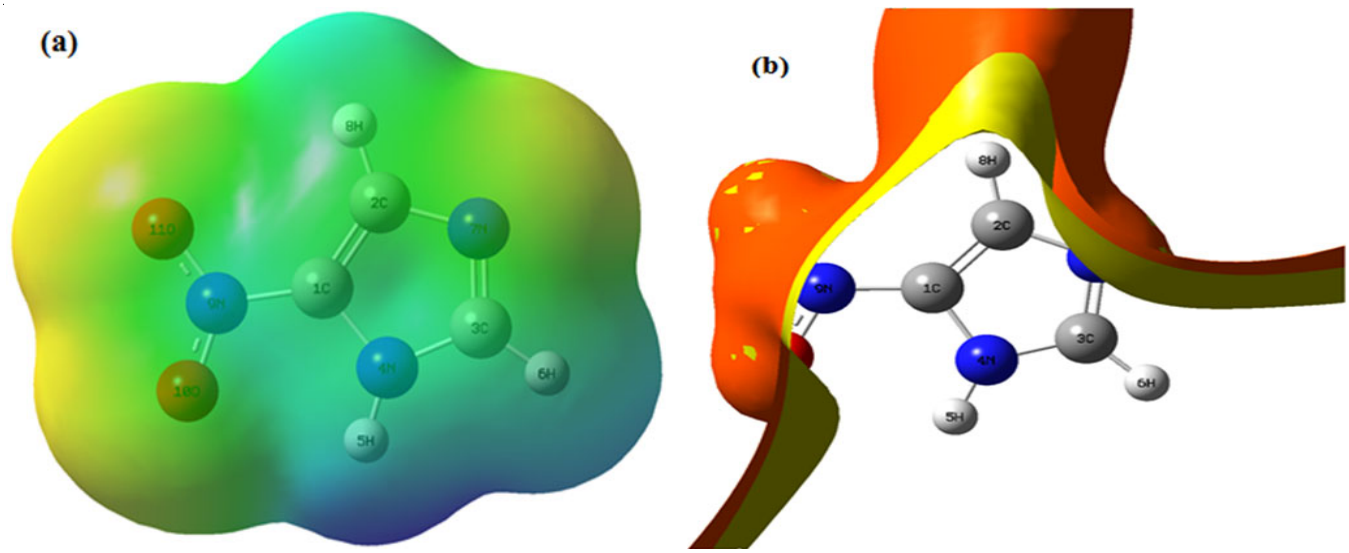

Fig. 6. (a) Molecular electrostatic potential (MEP); (b) Electrostatic potential (ESP) for 4-nitroimidazole

strongest attraction and oxygen atoms indicate the strongest repulsion.

Conclusion

The optimized parameters, wave numbers and intensities of vibrational bands of 4-nitroimidazole have been investigated using B3LYP/6-311++G(d,p) calculations along with the experimental spectra. The results of DFT-B3LYP method indicates better fit to experimental values. Furthermore, the total dipole moment and other thermodynamic properties have been calculated. The HOMO-LUMO energy gap and NBO analyses explains the intramolecular charge transfers which are responsible for biological activity. The Mulliken charge analysis explains the rearrangement of electron concentration in the molecule. The MEP surface predicts the relative reactivities towards electrophilic (hydrogen atoms) and nucleophilic (oxygen atoms) attacks. These results will be evidence for 4-nitroimidazole in pharmaceuticals and energy device applications.

CONFLICT OF INTEREST

The authors declare that there is no conflict of interests regarding the publication of this article.

REFERENCES

1. C.W. Ang, A.M. Jarrad, M.A. Cooper and M.A.T. Blaskovich, *J. Med. Chem.*, **60**, 7636 (2017); https://doi.org/10.1021/acs.jmedchem.7b00143
2. J. Zhang, Y. Ba, S. Wang, H. Yang, X. Hou and Z. Xu, *Eur. J. Med. Chem.*, **179**, 376 (2019); https://doi.org/10.1016/j.ejmech.2019.06.068
3. L. Minier Jr., R. Behrens and S. Bulusu, In eds.: T.B. Brill, T.P. Russell and W.C. Tao, Decomposition, Combustion and Detonation Chemistry of Energetic Materials, Materials Research Society, Pittsburgh, PA, vol. 418, p. 111 (1995).
4. X. Su, X. Cheng, C. Meng and X. Yuan, *J. Hazard. Mater.*, **161**, 551 (2009); https://doi.org/10.1016/j.jhazmat.2008.03.135
5. Z. Yu and E.R. Bernstein, *J. Chem. Phys.*, **137**, 114303 (2012); https://doi.org/10.1063/1.4752654
6. M. Mushtaque, F. Avecilla, A. Haque, Z. Yab, M.M.A. Rizvi and M.S. Khan, *J. Mol. Struct.*, **1185**, 440 (2019); https://doi.org/10.1016/j.molstruc.2019.02.101
7. Z. Zhou, D. Du, A. Fu and Q. Yu, *J. Mol. Struct. THEOCHEM*, **530**, 149 (2000); https://doi.org/10.1016/S0166-1280(00)00322-5
8. M.J. Frisch, G.W. Trucks, H.B. Schlegal, G.E. Scuseria, M.A. Robb, J.R. Cheesman, V.G. Zakrzewski, J.A. Montgomerg Jr., R.E. Stratmann, J.C. Burant, S. Dapprich, J.M. Millam, A.D. Daniels, K.N. Kudin, M.C. Strain, O. Farkas, J. Tomasi, V. Barone, R. Cammi, B. Mennucci, M. Cossi, C. Pomelli, C. Adamo, S. Clifford, J. Ochterski, G.A. Petersson, P.Y. Ayala, Q. Cui, K. Morokuma, N. Rega, P. Salvador, J.J. Dannenberg, D.K. Malich, A.D. Rabuck, K. Raghavachari, J.B. Foresman, J. Cioslowski, J.V. Ortiz, A.G. Baboul, B.B. Stetanov, A. Liashenko, G. Liu, P. Piskorz, I. Komaromi, R. Gomperts, R.L. Martin, D.J. Fox, T. Keith, M.A. Al-Laham, C.Y. Peng, A. Nanayakkara, M. Challacombe, P.M.W. Gill, B. Johnson, M.W. Wong, J.L. Andres, C. Gonzalez, W. Chen, M. Head-Gordon, E.S. Replogle and J.A. Pople, GAUSSIAN 09, Revision A 11.4, Gaussian, Inc., Pittsburgh PA (2009).
9. A.D. Becke, *J. Chem. Phys.*, **98**, 5648 (1993); https://doi.org/10.1063/1.464913
10. C. Lee, W. Yang and R.G. Parr, *Phys. Rev. B Condens. Matter*, **37**, 785 (1988); https://doi.org/10.1103/PhysRevB.37.785
11. M. Castella-Ventura, E. Kassab, G. Buntinx and O. Poizat, *Phys. Chem. Chem. Phys.*, **2**, 4682 (2000); https://doi.org/10.1039/b006459i
12. MOLVIB Version 7.0: Calculation of Harmonic Force Fields and Vibrational Modes of Molecules, QCPE Program No. 807 (2002).
13. I. Ségalas, J. Poitras and A.L. Beauchamp, *Acta Crystallogr. C*, **48**, 295 (1992); https://doi.org/10.1107/S0108270191008065
14. D.C. Young, Computational Chemistry: A Practical Guide for Applying Techniques to Real World Problems (Electronic), John Wiley & Sons Ltd.: New York (2001).
15. S. Gunasekaran, R.K. Natarajan and K. Santhosam, *Asian J. Chem.*, **15**, 1347 (2003).
16. V. Krishnakumar and R.J. Xavier, *Spectrochim. Acta A Mol. Biomol. Spectrosc.*, **60**, 709 (2004); https://doi.org/10.1016/S1386-1425(03)00281-6
17. S. Jeyavijayan, *Indian J. Pure Appl. Phys.*, **54**, 269 (2016).
18. M. Arivazhagan, S. Jeyavijayan and J. Geethapriya, *Spectrochim. Acta A Mol. Biomol. Spectrosc.*, **104**, 14 (2013); https://doi.org/10.1016/j.saa.2012.11.032
19. M. Arivazhagan and S. Jeyavijayan, *Indian J. Pure Appl. Phys.*, **49**, 516 (2011).
20. L. Padmaja, C. Ravikumar, D. Sajan, I. Hubert Joe, V.S. Jayakumar, G.R. Pettit and O. Faurskov Nielsen, *J. Raman Spectrosc.*, **40**, 419 (2009); https://doi.org/10.1002/jrs.2145
21. S. Gunasekaran, S. Kumaresan, R. Arunbalaji, G. Anand and S. Srinivasan, *J. Chem. Sci.*, **120**, 315 (2008); https://doi.org/10.1007/s12039-008-0054-8
22. E.D. Glendening, J.K. Badenhoop, A.E. Reed, J.E. Carpenter, J.A. Bohmann, C.M. Morales and F. Weinhold, NBO 5.0, Theoretical Chemistry Institute, University of Wisconsin, Madison, USA (2001).
23. J.S. Murray and K. Sen, Molecular Electrostatic Potentials, Concepts and Applications, Elsevier, Amsterdam, pp. 7–624 (1996).